Measurement of the K-shell photoionization cross section of C IV through the L-shell photoabsorption spectra

E. Jannitti
Istituto Gas Ionizzati del Consiglio Nazionale delle Ricerche, via Gradenigo 6/a, 35131 Padova, Italy

P. Nicolosi, P. Villoresi, and F. Xianping*
Dipartimento di Elettronica e Informatica, Università di Padova, via Gradenigo 6/a, 35131 Padova, Italy
(Received 7 February 1994)

The photoabsorption spectrum of the C IV ion has been obtained with the two laser-produced plasma technique. The $1s$ inner-electron and the $2s$ and $2p$ valence-electron absorption spectra have been measured. From the L-shell spectra the value of the line ion density in the $1s^2 2s$ and $1s^2 2p$ levels has been obtained and the measurement of the total inner-shell photoionization cross section has been derived. The absorption line profiles of the L-shell spectra have also been compared with the theories of line broadening due to the Stark effect.

PACS number(s): 32.80.Fb, 32.70.Cs, 32.70.Jz

INTRODUCTION

Absorption spectroscopy is a fundamental technique for studying the photoionization and autoionization atomic processes. In addition, it can provide more information than emission spectroscopy about the energetic structure of inner-shell and double-electron excitation atomic levels, and, in particular, is best suited for measuring oscillator strengths and photoionization cross sections of transitions arising from a discrete absorbing level (usually the ground level). Absorption spectroscopy, therefore, is specifically useful for testing the validity of theoretical calculations of atomic or ionic structure. Theoretical values of both oscillator strengths and photoionization cross sections are, in fact, rather sensitive to the chosen wave functions and to the approximations used, especially when electron correlation and relativistic effects must be taken into account. Unfortunately, in an absorption experiment, the quantity measured is the spectrum of the absorption coefficient that can be used to yield the product of the column density of atoms or ions in the absorbing level times the absorption oscillator strengths or the photoionization cross sections, depending on the transitions involved (bound-bound or bound-free). Therefore, these parameters can be evaluated on an absolute scale only by measuring independently the column (or line) density in the absorbing level. Various independent experimental methods exist for measuring accurately the column density of neutral or singly ionized absorbing matter [1], but the measurement is more difficult and less accurate for highly ionized matter, especially when more short-lived species with high-density gradients are simultaneously present, as in laser-produced plasmas.

However, the measurement of the column density is not required if the value of the oscillator strength of at least one transition from the absorbing level is well known, as measured in previous independent experiments. In this case absorption spectroscopy can be utilized as a diagnostic technique for deriving the column density from the measured absorption coefficient, and the spectrum can be normalized on an absolute scale. The same procedure can be applied if the parameter known is the photoionization cross section.

A similar procedure can be followed when only theoretical values of oscillator strengths or photoionization cross sections are known. In this case, the uncertainty of the measured values is strictly affected by the accuracy of the theoretical models. In general, the latter is very high for transitions of valence electrons in simple atomic or ionic systems, when a good model of the potential field, where the absorbing electron moves, is allowed. For example, apart from the hydrogenic system, whose parameters can be exactly calculated, for ions belonging to simple isoelectronic sequences (He-, Li-, Be-like) the theoretical models can provide results with small errors, particularly for strong electric dipole-allowed transitions. By considering that for ionized matter the measurement of column density and level population can be more difficult and less accurate than for neutral matter, this procedure can be particularly useful for diagnostic purposes in the analysis of simple highly ionized species. The same procedure cannot be applied to the analysis of complex atomic or ionic systems, because in these cases the theoretical models are less reliable and it is difficult to estimate the uncertainty of data derived from these models.

The column density, evaluated from the absorption coefficient measured for valence-electron transitions, can be utilized even for obtaining, on an absolute scale, the

*Present address: Shanghai Institute of Optics and Fine Mechanics, China.

oscillator strengths and photoionization cross section of inner-shell spectra, provided that the experimental conditions are kept unchanged.

In the present paper we report an absolute measurement of the photoionization cross section of the 1*s* inner electron of C IV in the spectral range 25–34 Å. The measurement has been obtained with two different inner-shell C IV absorption spectra. An old one, taken in the spectral range 25–44 Å, has been used to extend the measurement of the photoionization up to 25 Å. A new one, taken in the spectral range 33–44 Å, has been used to achieve the absolute value of the photoionization cross section at the ionization threshold ($\sim$34 Å). For this latter case, the required column density of the absorbing level 1*s* has been evaluated from two different absorption spectra of the valence electron, taken in the spectral range 200–250 Å, with the same experimental conditions. In fact, the 2*s* and 2*p* levels are both populated from the valence electron during the measurement, while the population in levels higher than 2*p* is negligible. Practically, the column density of the absorbing level 1*s* has been considered as sum of two contributions, differently identified by the level occupied from the valence electron. These two contributions have been evaluated by measuring the absorption coefficients of discrete transitions of the valence electron from these levels, and by using calculated oscillator strengths. In fact, for Li-like spectra it is possible in literature to find very accurate values of oscillator strengths calculated by theoretical methods like close-coupling and model potential methods, as well as by semiempirical calculations, since correlations between valence and inner electrons are negligible. These methods, applied to the strong dipole-allowed transitions of 2*s* and 2*p* valence electrons of C IV, provide essentially identical oscillator strength values, within an expected error of less than $\pm 10\%$ [2,3].

Once the column density of the absorbing plasma has been determined, the absolute value of the inner-shell photoionization cross section at the ionization threshold ($\sim$34 Å) has been evaluated by measuring the absorption coefficient with the new inner-shell spectrum. The extension from 34 up to 25 Å has been obtained by normalizing, to the absolute value at threshold, the relative trend derived from the old spectrum.

The absorption spectra have been obtained with the technique of the two laser-produced plasmas, one acting as absorbing ionized medium, the other as background continuum source. The technique permits one to measure the absorption spectrum of a single ion, among the different ones produced in the absorbing plasma. The problems concerning the applications of this technique have been exhaustively dealt with in previous papers [4,5], to which the reader is referred.

THE EXPERIMENT

The experimental technique has been extensively described in previous papers [4–6], and therefore only the principles of the experiment will be described here with details regarding the present measurements. The absorption spectra have been obtained by using two laser-produced plasmas, the first one acting as background continuum radiation source in the soft x-ray spectral range, the second one acting as absorbing medium. Figure 1 shows the optical scheme of the experiment. The instrument consists of a toroidal mirror *M* coupled with a spherical grating spectrometer, both working at grazing incidence. The toroidal mirror corrects the astigmatism of the grating *G* and fills its optimum aperture. In this way the luminosity of the instrument is greatly improved and the diffracted spectrum results quasistigmatic. Both the emitting and absorbing plasmas are generated from a split pulse of a ruby laser . This latter operates in the *Q*-switched regime and has up to 10 J of energy and 15-ns full width at half maximum (FWHM) of duration. About 70% of the laser energy has been sharply focused with an aspheric lens ($f=50$ mm, $f/1.4$) onto a plane tungsten (W) target *T*. The generated plasma emits a strong, short ($\sim$20 ns) and spectrally smooth continuum pulse of soft x rays [2]. The instrument looks directly inside the crater region, where the high value of the electron density causes the strong emission of soft x-ray radiation. A further advantage of this optical scheme is that, with a proper choice of the curvature radii of the toroidal mirror, the distances between the continuum source, the mirror itself, and the spectrograph can be kept quite large (some tens of centimeters) with obvious operational advantages. In Table I the main parameters of the experiment are reported. The absorbing plasma has been generated by focusing the second part of the laser beam onto a plane graphite (C) target *P*. A spherocylindrical lens was used in order to increase the length of the absorbing column and then the measured absorption. A suitable optical delay has been introduced between the two laser beams, in order to synchronize the crossing time of the continuum through the absorbing plasma. The focal spot size and the laser energy onto the C target have been optimized in order to give the expected ionization degree of the plasma. The C plasma was generated closely in front of the slit *S* of the spectrograph, and therefore only a small portion of the absorbing plasma was irradiated from the continuum radiation focused by the toroidal mirror. In this way effects due to the nonuniform density of the expanding plasma can be reduced and the probed portion of the plasma varied by moving the C target along its normal direction.

The detection system is shown schematically in Fig. 2. It consists of a plane fiberoptic faceplate S+FP sliding

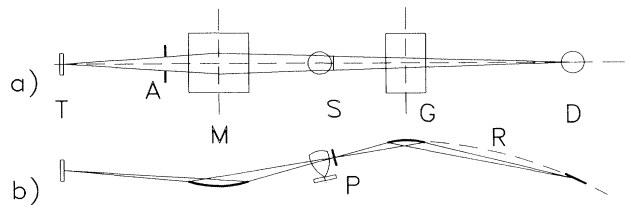

FIG. 1. Optical setup of the experiment: (a) sagittal view; (b) tangential view. *T*, target; *A*, aperture limiter; *M*, toroidal mirror; *S*, slit; *G*, grating, *P*, absorbing plasma; *D*, detector; and *R*, Rowland circle.

TABLE I. Experimental parameters.

Laser pulse: Energy 7 J, duration 15 ns.
Laser power density: on W target $\sim 2\times 10^{12}$ W/cm^2, on C target $\sim 4.5\times 10^9$ W/cm^2.
Focal spot size on C target: 0.7×2.8 mm^2.
Distance from the surface of the absorbing plasma: 0.6 mm.
Time delay between the laser pulses: 15 ns.
Toroidal mirror radii: equatorial $R=5600$ mm; sagittal $\rho=26$ mm.
Angle of incidence of the toroidal mirror: 87.3°.
Entrance slit width: ~ 8 μm.
Gratings: 1200 l/mm, Pt coated; 576 l/m Au coated.
Angle of incidence of the grating: 86°.
Aperture of the instrument: (1/600)+(1/120) [(sagittal)×(equatorial)].
Detector head: OMA EG&G 1450, photodiode linear array,
512 pixel of 25-μm spectral width.
Scintillator coating: P45 phosphor, 3-μm average grain diameter, 10–15-μm thickness.
Intensifier: Thompson mod. TH9304.

along the Rowland cylinder coated by a scintillator, 10–15 μm thick. The scintillator coating has been obtained by deposing, by a sedimentation technique, P45 phosphor grains of 3-μm average diameter. This latter provides efficient conversion from xuv to visible photons, and permits the use of standard optical elements to transfer the spectrum from the Rowland circle up to the photodiode array (PDA). The faceplate is coupled to a fiberoptic coherent flexible bundle B and then to a second faceplate sealed as a vacuum window. In air there is an image intensifier (I.I.), coupled to the faceplate vacuum window, whose output is focused with higher luminosity (f/0.8) objectives on the photodiode array.

The absorption coefficient $k(\lambda)$ is obtained by

$$k(\lambda)=\ln\left[\frac{I_0(\lambda)}{I(\lambda)-I_e(\lambda)}\right], \tag{1}$$

where $I_0(\lambda)$ and $I(\lambda)$ are the continuum intensities incident on and transmitted through the absorbing plasma, while $I_e(\lambda)$ is the intensity emitted from the absorbing plasma itself. Several exposures are accumulated for reducing the statistical shot-by-shot fluctuations and for increasing the signal-to-noise ratio. While in the case of a continuous spectrum the measured absorption coefficient according to Eq. (1) is not affected by the finite instrumental resolving power; on the contrary, for discrete line spectrum the influence of the finite instrumental resolving power on the measured absorption spectrum is generally quite strong and nonlinear. For this reason a deconvolution procedure must be applied in order to recover the true absorption coefficient. On the other hand, the instrumental function can be determined independently by observing very narrow line profiles both in emission and in absorption.

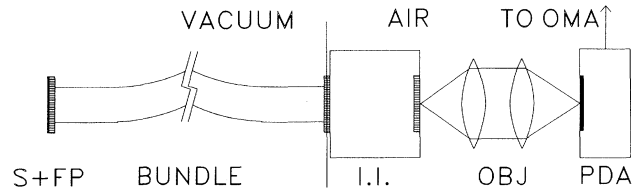

FIG. 2. Schematic of the detector: S+FP, plane fiberoptic faceplate with scintillator coating; BUNDLE, coherent fiberoptic bundle, I.I, image intensifier; OBJ, optical coupling via high aperture objective pair; and PDA photodiode array.

The absorption coefficient of a discrete line is given by

$$k(\lambda)=\frac{\pi e^2\lambda^2}{mc^2} f\phi(\lambda)\int_1 n\,dl\ , \tag{2}$$

where f is the absorption oscillator strength, $\phi(\lambda)$ is the normalized intrinsic line profile, and $\int_1 n\,dl$ is the line density through the absorbing column. On the other hand, the absorption coefficient of the continuous spectrum is given by

$$k_c(\lambda)=\sigma(\lambda)\int_1 n\,dl\ , \tag{3}$$

where $\sigma(\lambda)$ is the photoionization cross section and $\int_1 n\,dl$ is the line or column density of ions in the lowest level of the transition. From Eqs. (2) and (3) it is clear that $\sigma(\lambda)$ can be evaluated by measuring $k_c(\lambda)$ and deriving the $\int_1 n\,dl$ value from measurements of $k(\lambda)$ of lines with known oscillator strength.

The purpose of the present experiment is to determine the photoionization cross section $\sigma(\lambda)$ of the C IV inner-shell spectrum. The line density to be used in Eq. (3) has been derived by measuring the absorption coefficient of some discrete lines of the valence electron. For this spectrum there are no experimental determinations of oscillator strength. However, due to its simple Li-like electron structure, the theoretical calculations are accurate and reliable. The searched line density is yielded through Eq. (2) and used, then, with the absorption coefficient measured for the inner-shell spectrum.

Since these spectra are at considerably different spectral ranges, the spectrograph was equipped with two gratings, easily interchangeable by a cinematic grating holder. The inner-shell spectrum was observed with a 1200-l/mm grating blazed at about 40 Å, while the valence-electron spectrum has been observed mounting a 576-l/mm grating blazed at about 200 Å. The change of the gratings was accomplished keeping strictly constant the

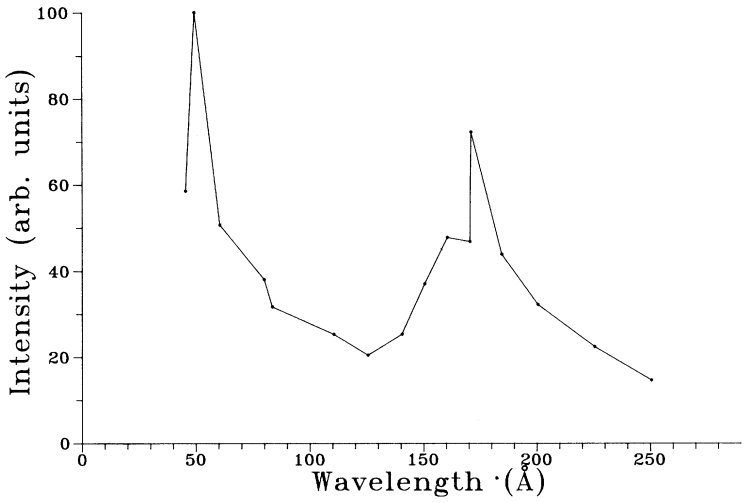

FIG. 3. Relative continuum emission from a tungsten plasma observed through Al filter (1000 Å of thickness).

other experimental parameters. However, in deriving the absorption spectra in the two cases the different contribution of the high diffraction orders must be considered. For the inner-shell spectrum, the diffraction efficiency of the instrument drops abruptly below 25 Å, because of the decrease at the shortest wavelengths of the efficiency of the grating, working at 86° angle of incidence, and of the reflectivity of the toroidal mirror. Therefore, the inner-shell spectrum in the range of 25–45 Å is free from high-order contributions. On the other hand, the efficiency of the instrument configured for the valence-electron spectrum decreases slowly on the short-wavelength side, i.e., below 200 Å, and this absorption spectrum is found to be strongly affected by high diffraction orders. In order to derive a correction curve for the measured continuous spectrum, the true diffraction efficiency of the 576-l/mm grating has been measured by observing B, C, and N resonance emission lines up to the fifth order. For this purpose, a few gratings have been tested, and the one having the lowest contribution from higher orders has been selected. In addition, in order to reduce this unwanted contribution, an Al filter, about 1000 Å thick, has been placed on the optical path in front of the grating. Nevertheless the detected signal remained strongly affected by these contributions, which ranged from about 20% at 180 Å up to 60% at 250 Å of the measured intensity.

In Fig. 3 the relative continuous emission from the tungsten plasma, observed with the low dispersion grating, is reported. The *L*-edge absorption of Al is clearly visible at 170 Å; on the other hand, a significant increase of transmission of the filter has been observed at shorter wavelengths. Both the background continuous spectrum $I_0(\lambda)$ and the absorption spectrum $I(\lambda)$ have been corrected for the higher-order contributions, assuming that the higher-order continua are not modified by the absorbing plasma.

THE C IV SPECTRUM

A simplified energy-level diagram of C ions is reported in Fig. 4. The C IV spectrum in the extreme ultraviolet (EUV) region consists essentially of the valence- and inner-shell-electron spectra. Both correspond to transitions starting from the ground and low excited levels: $1s^2 2s$ and $1s^2 2p$, but have transition energies quite different. In the figure the first members of these spectra are shown with their corresponding wavelengths in angstroms. In fact, the final states of the valence-electron spectrum are below the ionization limit, while those of the inner electron are doubly excited states above the ionization limit. The former ones correspond to the series $1s^2 2s\ ^2S - 1s^2 np\ ^2P$ with an ionization limit at 192.2 Å, and to the series $1s^2 2p\ ^2P - 1s^2 ns\ ^2S$, $1s^2 nd\ ^2D$, both converging to the same limit at 219.5 Å. The latter ones correspond to transitions $1s^2 2s - 1s2lnl'$, the limits $1s2s\ ^1S$ and $1s2p\ ^{1,3}P$ being at about 34 Å. While many theoreti-

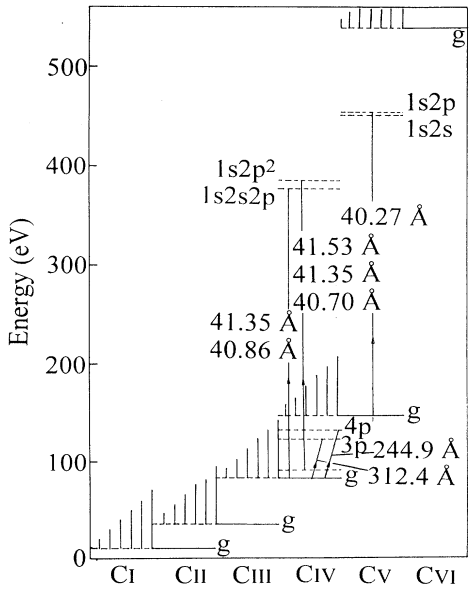

FIG. 4. Level diagram for the *K*- and *L*-shell transitions of C ions.

cal and experimental studies have been published about the Li-like spectrum of carbon, very few data have been reported for the doubly excited spectrum. In particular, it is worthwhile to mention the works of Peach, Saraph, and Seaton [5] and Drew and Storey [6], where the photoionization cross sections of the C IV are reported, and those of Biemont [7], Martin and Wiese [8], and Lindgard and Nielsen [9] which report oscillator strength calculations. The inner-shell spectrum of carbon has been studied by Gabriel [10], who calculated energies of some doubly excited states of the type $1s2l2l'$. These lines appear on the long-wavelength side of the $1s^2-1snp$ resonance lines of the He-like C V and are called satellite lines. Since these states can be populated by inner-shell excitation from the Li-like ground state or by dielectronic recombination of He-like ions, these lines, observed in emission, can be used for plasma diagnostics. Doubly excited spectra of C IV emitted by laser-produced plasmas have been studied by Peacock, Hobby, and Galanti [11] and Nicolosi and Tondello [12]. More recently our group (Jannitti, Nicolosi, and Tondello [13]) has reported on $1s$ electron absorption spectra of carbon ions. There the C IV absorption has been obtained with the present experimental technique, in the spectral range 25–44 Å. That spectrum is reported in Fig. 5 and was achieved with a 4×10^9-W/cm^2 laser power density on a 0.9×1.2-mm^2 focal spot area onto the carbon target; the carbon plasma was probed by the background continuum at 1.1 mm from the target surface, with a delay of 30 ns. The experimental parameters were chosen in order to obtain the best resolution with respect to the adjacent C V and C III ionization stages. This was really a very difficult task; indeed, a few strong C III absorption lines appear at about 42 Å, and the C V resonance lines are also evident. The absorption coefficient in the discrete portion of the spectrum was obtained through deconvolution with the instrumental function. For this purpose, a constrained deconvolution process was applied to the absorbance, which is defined as $1-I(\lambda)/I_0(\lambda)$, where $I(\lambda)$ and $I_0(\lambda)$, respectively, are the transmitted and incident background continuum intensities, and is constrained between extreme values of 0 and 1 [14]. The instrumental function was independently measured and found to be influenced mostly by the resolution of the detection system. Most of the discrete lines have been identified as $1s^22s-1s2snp$ and $1s^22p-1s2pnp$ transitions [15], and members up to $n=6$ have been observed. The continuous inner-shell absorption was measured up to 25 Å and was fitted (dotted line) with the theoretical calculations of Reilman and Manson [16], normalized to the threshold experimental value. Excellent agreement between experimental and theoretical data within their uncertainties was observed only for a few angstroms above the ionization limit, while at higher energies some contribution from C V photoionization was superimposed on the C IV one. This contribution, suitably normalized to the difference between the experimental result and the theoretical calculation of Reilman and Manson at the C V ionization limit, was determined from C V photoionization absolute measurements reported in Ref. [17]. The removal of this contribution from the experimental result made it possible to obtain the relative photoionization cross section of the C IV up to 25 Å. An absolute value for this spectrum was not derived from the measured absorption coefficients, because the line density of C IV ions in the lower states was unknown.

Indeed, Drew and Storey have calculated the photoionization of C IV from the ground state $1s^22s\ ^2S$, extended far enough to include the inner-shell photoionization [6]. In particular they report the cross sections for the $1s2s3l$ and $1s2p3l$ groups of resonances. Unfortunately, it was not possible to derive the line density accurately using the calculated oscillator strengths, because the experimental profiles of the very sharp inner-shell resonances were found to be strongly affected by the finite instrumental resolution, and the absorption coefficients were strongly dependent on the deconvolution process.

In the present experiment we have used the transitions of the valence electron for deriving the line density of C IV ions according to Eq. (2) and consequently the absolute value of the inner-shell cross section. In fact these transitions are only weakly affected by the finite instrumental resolution, and the true absorption coefficients can be determined very accurately. Moreover the oscilla-

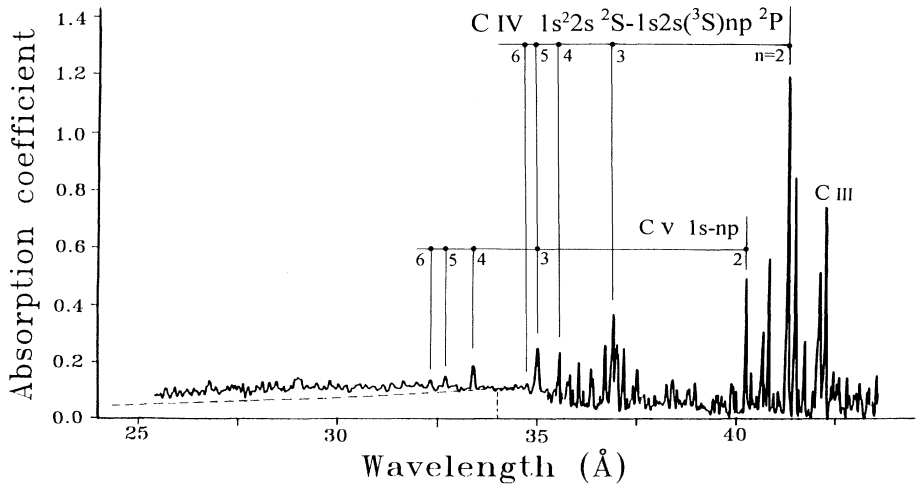

FIG. 5. C IV K-shell absorption spectrum. Plasma conditions indicated in the text.

tor strengths of transitions of the valence electron in Li-like ions have been calculated with high accuracy, to within 5–10 % [5,6].

The new inner-shell spectrum between 33 and 44 Å, performed for evaluating the absolute value at threshold of the inner-shell photoionization, has been obtained with the experimental parameters reported in Table I and is shown in Fig. 6. It has been taken with the highest dispersion grating in order to achieve the best spectral resolution and the highest efficiency. In addition, the experimental parameters have been adjusted in order to achieve a measurable jump at the ionization threshold. The discrete spectrum is essentially like that reported in the previous Fig. 5. Only the C V and C III relative contributions and the absorption coefficient values are different. Since our interest is in the threshold transition between the discrete and the continuous absorption spectra, in this case the constrained deconvolution procedure has not been applied. The absorption coefficient value at the threshold is found to be $k=0.1$, and is given by the absorption from both $1s^2 2s$ and $1s^2 2p$ states, according to

$$k = n(2s)\sigma_s + n(2p)\sigma_p \ , \tag{4}$$

where $n(2s)$ and $n(2p)$ are the C IV line densities on the two levels, and σ_s and σ_p are the corresponding inner-shell photoionization cross sections. The valence-electron spectra have been taken in the same experimental conditions, i.e., laser power density, distance from the C target, focal spot size, delay. However, the spectrograph mounted the grating with the highest efficiency around 200 Å. The absorption coefficient, derived after the correction for the emission contribution from the absorbing plasma and for the higher diffraction orders of the continuous spectra, is reported in Figs. 7 and 8. In Fig. 7 are shown the lines $1s^2 2s\ ^2S - 1s^2 np\ ^2P$ with $n=5$, 6, and 7, and in Fig. 8 the lines $1s^2 2p\ ^2P - 1s^2 nd\ ^2D$ with $n=6$, 7, and 8. Also in Fig. 8 the $1s^2 2s\ ^2S - 1s^2 4p\ ^2P$ line appears on the short-wavelength wing of the $1s^2 2p\ ^2P - 1s^2 6d\ ^2D$ line. The absorption for this line is very strong, and saturation is evident. Because of the reduced intensity of the background continuum, due to the relatively low efficiency of the spectrograph at these wavelengths, these spectra are also more affected by the noise. Therefore up to 200 acquisitions were needed for each spectrum to provide a good signal-to-noise ratio, that was larger for the *2s-np* series than for the *2p-nd* one; the latter also shows broader line profiles. The $1s^2 2p\ ^2P - 1s^2 ns\ ^2S$ series has not been observed. In fact, the corresponding oscillator strengths are considerably smaller.

Some background absorption is present in both the reported spectra. We suppose it could be due to some C III contribution as well as to some systematic effects, e.g., in performing the higher-order contribution correction. However this background absorption does not affect the measurements because the photoionization cross sections have been evaluated with respect to this background level.

The experimental line profiles have been fitted with Voigt profiles as shown in the Figs. 7 and 8. In the best fit the FWHM and the area of the profiles were free parameters, the former affecting mostly the shape and the latter the value of the absorption. The synthetic spectrum has been converted to absorbance and a constrained deconvolution procedure has been applied, taking into account the instrumental function width. The true absorption coefficient, i.e., without the distortion due to the finite instrumental resolution, is obtained when the deconvoluted absorbance is reconverted to k, and is reported in Figs. 9 and 10 for the corresponding spectra. Clearly the broad *2p-nd* profiles are less affected by the finite instrumental resolution. Since the area of the absorption coefficient profiles is proportional to the product of the absorption oscillator strengths times the line densi-

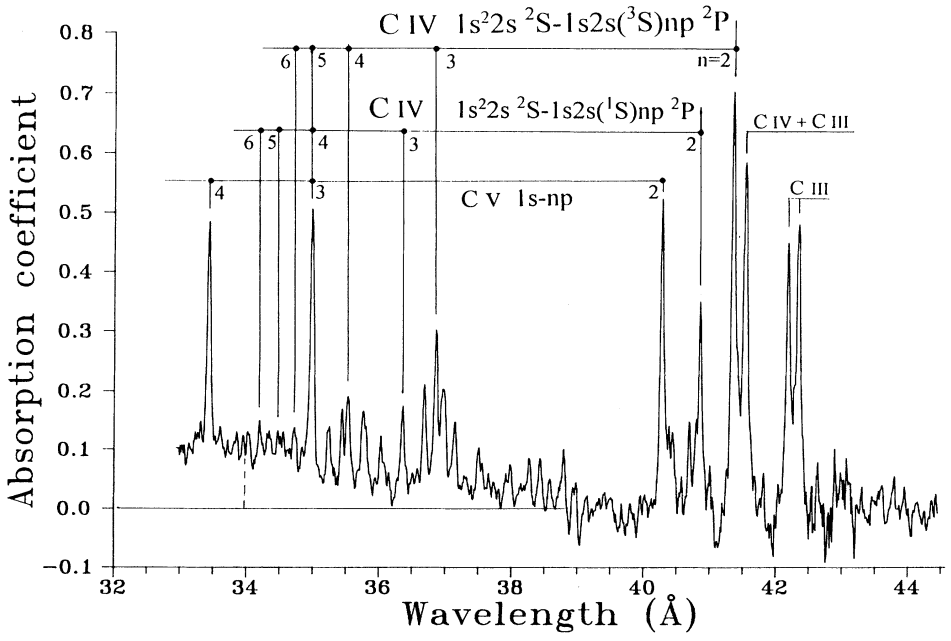

FIG. 6. C IV *K*-shell absorption spectrum obtained with parameters as in Table I.

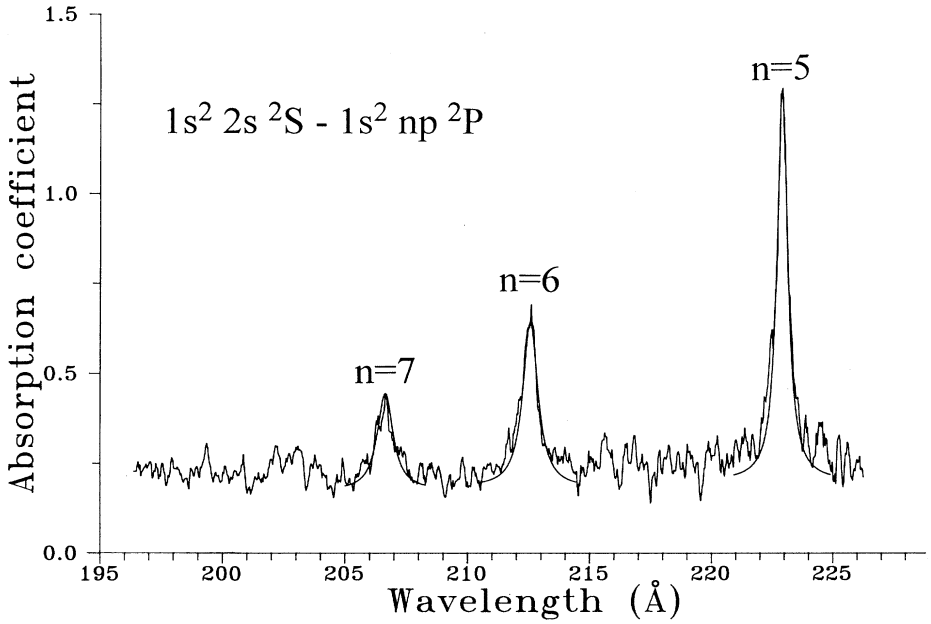

FIG. 7. C IV L-shell absorption spectrum from 196 to 225 Å with best-fit profiles obtained from a synthetic spectrum using Voigt line profiles.

ty of ions on the lower level according to Eq. (2), from the knowledge of the f values and the area of the profiles it is possible to derive the line density. The corresponding values for the C IV ions in the $1s^2 2s$ and $1s^2 2p$ levels, respectively, are $n(2s)=(7.6\pm1.0)\times10^{16}$ cm^{-2} and $n(2p)=(9.2\pm1.1)\times10^{16}$ cm^{-2}. The error bars for these measurements are due mostly to the uncertainty in the estimate of the higher-order contributions, and are asymmetric, due to their nonlinear incidence. The value of the inner-shell photoionization cross section can now be derived, assuming that it essentially is not affected by the outer-shell electron, i.e., $\sigma_s \approx \sigma_p$. From Eq. (3) we derive an average value $\sigma^*=(0.6\pm0.1)$ Mb at the threshold ($\sim$34 Å). In Fig. 11 the theoretical photoionization cross section for the $1s$ inner electron is reported as given by Reilman and Manson [16]. The presently derived experimental measurement at threshold is also reported, with an error bar given according to the uncertainty in the line density evaluations. In the same figure are reported some experimental values at higher energy, as determined from the old inner-shell spectrum, by normalizing the relative photoionization to the actual absolute value at threshold. The agreement with the theoretical calculations appears very good.

STARK BROADENING OF C IV LINES

In our experimental conditions, the absorption line profiles of discrete transitions of the valence electron of

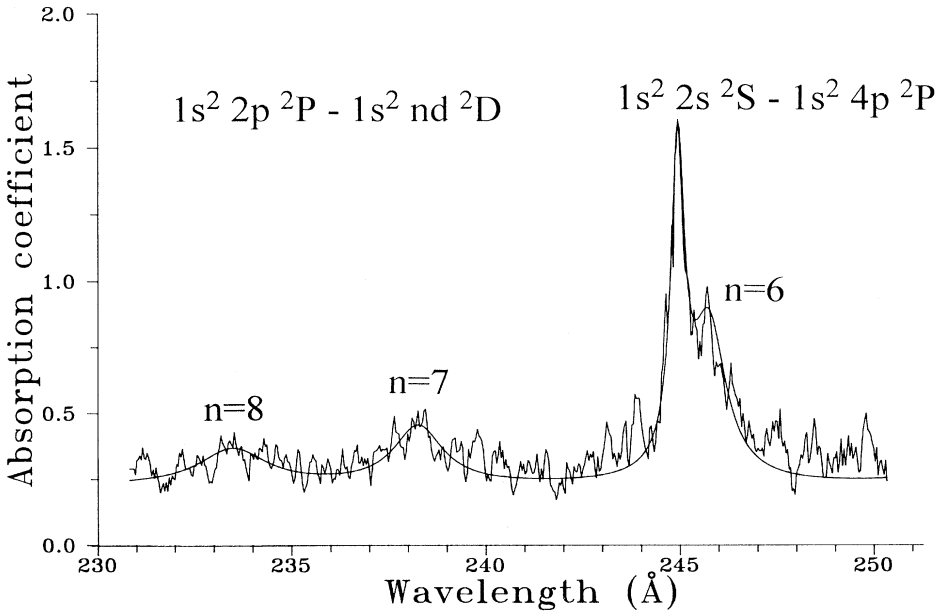

FIG. 8. C IV L-shell absorption spectrum from 230 to 250 Å with best-fit profiles obtained from a synthetic spectrum using Voigt line profiles.

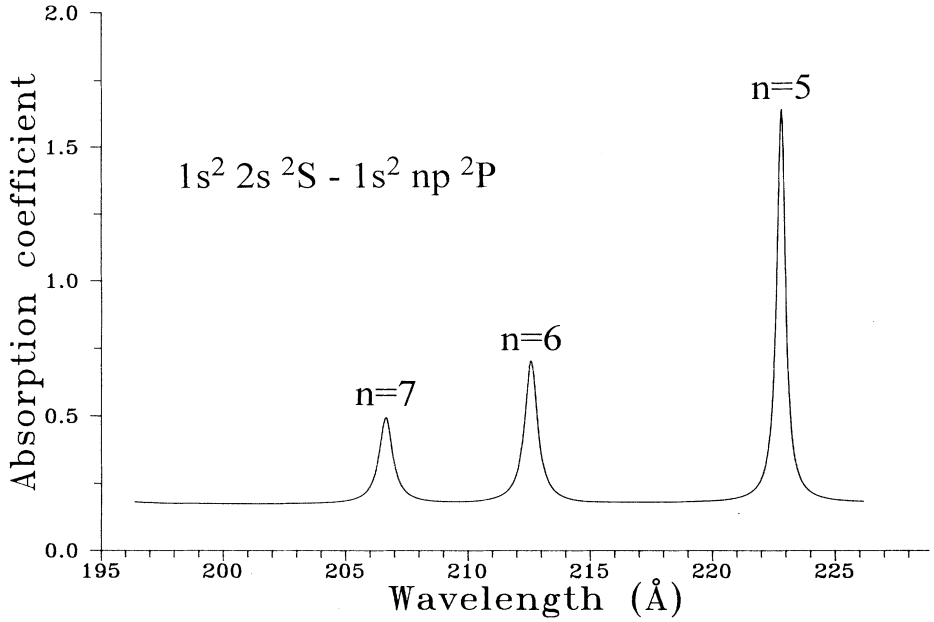

FIG. 9. Deconvolution of the absorption spectrum shown in Fig. 7.

the C IV ion appear broadened; in particular, the $2p$-nd lines are more broadened than the $2s$-np ones. The absorption line profiles of the deconvoluted spectra correspond to the intrinsic line profiles and are, therefore, well suited to testing the line broadening theories. In the plasma the main broadening mechanisms are usually the Stark and Doppler effects. In the present case the thermal Doppler broadening can be neglected, as well as the Doppler shift due to the expansion of the plasma. In fact, the plasma temperature is relatively low, and the elongated line focusing on the laser has the effect of reducing the longitudinal expansion of the plasma. In conclusion, the Stark effect seems to be the main broadening mechanism. It is interesting to compare the measured FWHM's of the observed lines with those that can be derived from the Stark broadening theory.

For this purpose, it is necessary to estimate the electron density of the absorbing plasma. From the absorption profile of the $1s^2$-$1s3p$ and $1s^2$-$1s4p$ lines of C V that are present in the inner-shell C IV spectrum reported in Fig. 5, and through Eq. (3), it is possible to derive the line density of C V ions in the ground state $1s^2\,{}^1S$. Using the oscillator strength values reported by Dalgarno and Parkinson [18], we can estimate a line density

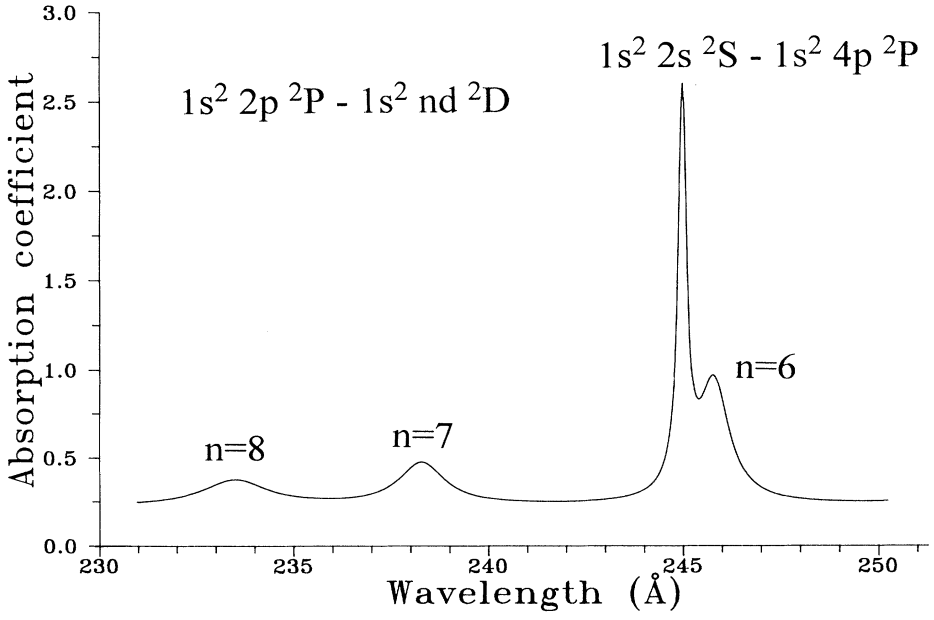

FIG. 10. Deconvolution of the absorption spectrum shown in Fig. 8.

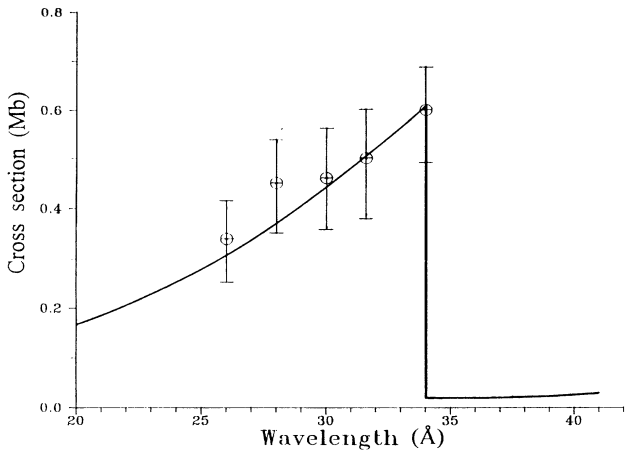

FIG. 11. K-shell photoionization cross section of C IV: comparison of the theoretical calculation of Reilman and Manson (solid line) with the experimental measurements.

$n(\mathrm{C\,V})=4.9\times10^{16}$ cm^{-2}. On the other hand, for the lines of the C III ion that appeared in the inner-shell spectrum, the values of the oscillator strength are not available. However, a rough estimation of the upper limit of the C III line density can be derived from the photoabsorption spectrum of Fig. 6. In fact, in the region where the C III ion should show continuous photoabsorption, only a faint contribution is apparent. This can be estimated, at maximum, as 20% of that of the C IV ion that has, in the same region, the discrete part of its spectrum. From the calculated inner-shell photoabsorption cross-section value $\sigma=0.76$ Mb, the upper limit for the line density can be estimated, therefore, as $n(\mathrm{C\,III})\leq 2.6\times10^{16}$ cm^{-2}.

Assuming that all these ions are present uniformly through the plasma, it is possible to derive, from the neutrality condition, the value of the electron line density integrated along the plasma:

$$\int_l n_e dl = 4n(\mathrm{C\,V})+3n(\mathrm{C\,IV})+2n(\mathrm{C\,III}) . \quad (5)$$

In Eq. (5) we have assumed that the contributions from bare nuclei, H-like and singly ionized ions are negligible. The value of n(C IV) takes into account that the ion population is mostly distributed between the two lowest states $1s^2 2s$ and $1s^2 2p$, while, for both C V and C IV, the population in the excited states can be neglected. From the laser spot size on the carbon target, the distance from the target of the probed plasma and the time elapsed from its generation, we have estimated an equivalent length of the plasma column of 2.7 mm, from which results an electron density of $n_e=2.7\times10^{18}$ cm^{-3}.

The population of C IV ions that has been derived is distributed between the $1s^2 2s$ and $1s^2 2p$ levels, assuming Boltzmann equilibrium at an electron temperature T_e of a few eV. The criterion for validity of the local thermodynamic equilibrium (LTE) approximation imposes $n_e \geq 2.6\times10^{17}$ cm^{-3} [19] and, consequently, is well satisfied. The time evolution of the plasma has not been taken into account. In Table II are reported the experimental values for the line broadening, together with the theoretical ones derived with the hydrogenic formula of Irons [20] and those, calculated by Griem, derived from the extrapolation of the profiles of ionized He [19].

TABLE II. Stark broadening of C IV lines.

	$\Delta\lambda_{\mathrm{Irons}}$ (Å)			$\Delta\lambda_{\mathrm{expt}}$ (Å)	
n_1-n_u	s-p	p-d	$\Delta\lambda_{\mathrm{Griem}}$ (Å)	s-p	p-d
2-5	0.15	0.20	1.08	0.39	
2-6	0.20	0.27	1.67	0.47	0.95
2-7	0.27	0.36	2.16	0.65	1.33
2-8		0.46			1.69

The Irons formula has been corrected by a factor of 2, according to the analysis of the experimental results reported by the same author [20]:

$$\Delta\lambda_{\mathrm{Irons}}(\text{Å})=\frac{8.11\times10^{-19}}{2}\frac{Z_p^{1/3}\lambda^2(\text{Å})}{Z}\tfrac{1}{2}(n_u^2-n_1^2)\times n_e^{2/3}(\mathrm{cm}^{-3}) . \quad (6)$$

Griem's estimate for the linewidth has been scaled to the actual ion charge according to Z^{-5}, with the following relation:

$$\Delta\lambda_{\mathrm{Griem}}(\text{Å})=2.5\times10^{-9}\alpha_{1/2}Z_p^{1/3}Z^{-5}n_e^{2/3}(\mathrm{cm}^{-3}) . \quad (7)$$

In the formulas, Z_p is the perturber charge, $Z=4$ is the effective atomic number, n_u and n_1 are the quantum numbers of the upper and lower levels of the transition, and $\alpha_{1/2}$ is the Holtsmark parameter of the calculated $S(\alpha)$ profile.

The values derived with the Irons formula are considerably different from the observed ones. This formula is based on the Holtsmark approximation and is valid only at relatively low densities, where Debye screening for electrons and ion-ion interaction are negligible. Therefore, comparison with the measurements allows one to conclude that, in the actual plasma conditions, such a hypothesis is not verified. On the other hand, the agreement with the values derived by extrapolating the Griem calculations is fairly good. In particular, the $2p$-nd lines have FWHM values well within 70% of the experimental ones. Moreover, the better agreement with the measurements of the p-d transitions in respect to the s-p ones can be explained by the fact that the outer shells are more similar to those of the hydrogenlike ions, on which the Griem model is based. For the p-d transitions, in fact, the line broadening is comparable to the energy separation of the levels.

CONCLUSIONS

By using the two laser-produced plasma photoabsorption technique in two different spectral ranges, we have been able to provide the photoionization cross-section value for inner-shell C IV in the spectral range 25–34 Å, obtaining excellent agreement with theoretical calculations of Reilman and Manson. For this purpose, the

column density of the plasma has been obtained from the absorption coefficients of valence-electron transitions in the spectral range 200–250 Å, and using accurate theoretical values of oscillator strengths. The comparison of the experimental line broadening with the Griem formula also shows a good agreement.

ACKNOWLEDGMENTS

The authors wish to thank Professor G. Tondello for many helpful discussions. One of the authors (F.X.) was supported by the International Centre for Theoretical Physics (Trieste, Italy).

[1] M. C. E. Huber and R. J. Sandeman, Rep. Prog. Phys. **49**, 397 (1986).
[2] G. Peach, H. E. Saraph, and M. J. Seaton, J. Phys. B **21**, 3669 (1988).
[3] J. E. Drew and P. J. Storey, J. Phys. B **15**, 2357 (1982).
[4] E. Jannitti, P. Nicolosi, and G. Tondello, in *X-Ray and VUV Interaction Data Bases, Calculations and Measurements,* edited by N. K. Del Grande, Proc. SPIE, Vol. 911 (SPIE, Bellingham, 1988), p. 157.
[5] E. Jannitti, M. Gaye, M. Mazzoni, P. Nicolosi, and P. Villoresi, Phys. Rev. A **47**, 4033 (1993).
[6] E. Jannitti, P. Nicolosi, and G. Tondello, Phys. Scr. **36**, 93 (1987).
[7] E. Biémont, Astron. Astrophys. Suppl. **27**, 489 (1977).
[8] G. A. Martin and W. L. Wiese, J. Phys. Chem. Ref. Data **5**, 537 (1976).
[9] A. Lindgard and S. E. Nielsen, At. Data Nucl. Data Tables **19**, 533 (1977).
[10] A. H. Gabriel, Mon. Not. R. Astr. Soc. **160**, 99 (1972).
[11] N. J. Peacock, M. G. Hobby, and M. Galanti, J. Phys. B **6**, L298 (1973).
[12] P. Nicolosi and G. Tondello, J. Opt. Soc. Am. **67**, 1033 (1977).
[13] E. Jannitti, P. Nicolosi, and G. Tondello, Phys. Scr. **41**, 458 (1990).
[14] P. A. Jansson, *Deconvolution with Application in Spectroscopy* (Academic, New York, 1984).
[15] M. Mazzoni (private communication).
[16] R. F. Reilman and S. T. Manson, Astrophys. J. Suppl. **40**, 815 (1979).
[17] E. Jannitti, P. Nicolosi, and G. Tondello, Phys. Lett. A **131**, 186 (1988).
[18] A. Dalgarno and E. M. Parkinson, Proc. R. Soc. London Ser. A **301**, 253 (1967).
[19] H. R. Griem, *Spectral Line Broadening by Plasmas* (Academic, New York, 1974).
[20] F. E. Irons, J. Phys. B **6**, 1562 (1973).